POLITEHNICA UNIVERSITY OF BUCHAREST
FACULTY OF MECHANICAL ENGINEERING AND MECHATRONICS
DOCTORAL SCHOOL
MACHINE ELEMENTS AND TRIBOLOGY DEPARTMENT

DOCTORAL THESIS
—ABSTRACT—

A COMBINED THEORETICAL AND EXPERIMENTAL STUDY OF THE TRIBOLOGY OF HUMAN SKIN WITH APPLICATIONS TO DIRECT AND INDIRECT MANIPULATION OF OBJECTS

AUTHOR**: ANDREI CĂLIN**

DOCTORAL COMITTEE

PRESIDENT	**PROF. DR. ING. RADU CHIRIAC**	**POLITEHNICA UNIVERSITY OF BUCHAREST**
SUPERVISOR	**PROF. DR. ING. ANDREI TUDOR**	**POLITEHNICA UNIVERSITY OF BUCHAREST**
REVIEWER	**PROF. DR. ING. DUMITRU OLARU**	**„GHEORGHE ASACHI” TECHNICAL UNIVERSITY IASI**
REFERENT	**CONF. DR. ING. FLORIN MUNTEANU**	**"GRIGORE T. POPA" UNIVERSITY OF MEDICINE AND PHARMACY, FACULTY OF MEDICAL BIOENGINEERING IASI**
REFERENT	**PROF. DR. ING. SORIN CĂNĂNĂU**	**POLITEHNICA UNIVERSITY OF BUCHAREST**

Bucharest, 2022

Acknowledgments

I have had the privilege of having Professor Andrei TUDOR as my PhD supervisor. I am deeply grateful for your advice, support, scientific expertise, and above all, your consistent encouragement. There are not enough words of gratitude to express all my admiration for you.

I would like to convey my thanks to the members of the doctoral committee for the support, advice and time given during my doctoral studies, prof. dr. eng. Sorin CĂNĂNĂU, prof. dr. eng. Petre Lucian SEICIU and assoc. prof. dr. eng. Georgiana CHIȘIU.

I thank the official referees for the time devoted to the analysis of the thesis, for the appreciations and efforts they made to assist the public support.

I express my gratitude to the entire team of the Department of Machine Elements and Tribology. Thank you for the support and trust I felt. Thanks to your support, I was able to overcome all the obstacles on the way to my goal.

I want to thank my friends for their constant support. I honestly doubt I could have finished without them. You all are a wonderful gift to me.

I would like to express my gratitude to my family, especially my mother, father, brother and grandmother, for everything.

KEY WORDS: Friction on human skin, Modeling human finger, Biotribology, Stick-Slip

OBJECTIVES

The doctoral thesis presents theoretical and experimental studies to determine the behaviour of human skin, in this case the papillary region, results that contribute to the fundamental understanding of the interaction between humans and objects. This information can be used and integrated directly in the early phase of product development to improve the manipulation of objects.

The objectives of the thesis can be summarised as follows:

- Identifying the current state of research on the tribological study of human skin. **(Chapter 1)**
- Theories used to model the state of stresses and strains at the viscoelastic contact of human fingers with bodies of simple geometry (plane, cylinder, sphere); Anisotropy analysis of human finger skin. **(Chapter 2)**
- Determining finger geometry and 3D scanning of a human finger and making a FEM model for modeling the human finger. **(Chapter 3)**
- Experimental studies on the "Stick-Slip" stand and on the CETR UMT-2 experimental stand of the Department of Machine Elements and Tribology and the determination of material characteristics for human skin using employing the indenter method on the CETR UMT-2 experimental stand. **(Chapter 4)**
- Theoretical model regarding the stick-slip phenomenon of the contact of the human finger with rigid artificial surfaces taking creep into account. **(Chapter 5)**

SINTHETIC PRESENTATION OF THE CHAPTERS OF THE DOCTORAL THESIS

Chapter 1 of the thesis presents generalities regarding the study of friction on human skin. The word "biotribology" was first used by Dawson and Wright in 1973 to describe aspects of tribology with respect to biological systems (Dawson, et al., 1973).

Currently, biotribology is one of the subfields of tribology with an increasing rate of scientific papers. The graph below represents the number of scientific studies with the keywords "Tribology" and "Biotribology" + "Bio tribology" present on ScienceDirect.com as of 01/06/2022. The data were collected for the period 1998-2022.

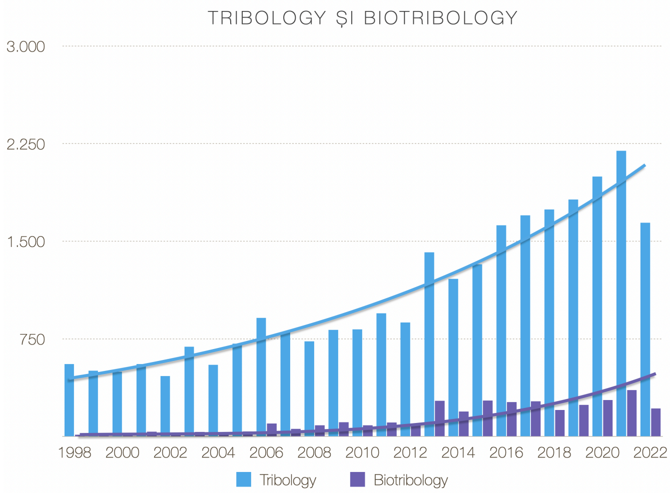

Figure 1.1 Evolution of the number of scientific studies in the last 22 years that have the keywords "Tribology" and "Biotribology"

The skin is a complex multifunctional organ that covers the entire surface of the body. To facilitate body movements, the skin must be flexible enough to take large deformations in all directions and at the same time return to its original shape. These functions require a wide range of mechanical properties. The structure of the skin can be divided into three layers. Starting from the outside, the skin can be divided into epidermis, dermis and hypodermis. The average total skin surface is 1.8 m^2, with an average thickness of 1.2 mm and a weight of 4.2 kg. The ratio between surface and thickness is approx. 150,000 (Agache, et al., 2004). Mosteller calculates the skin area to be approximately 2 m^2 (Mosteller, 1987). Richard revises the previous measurements to 25 m^2 justifying his calculation by the fact that the skin is not a flat surface but contains structures like hair follicles or sweat gland openings that increase the epithelial surface considerably (Richard, 2017).

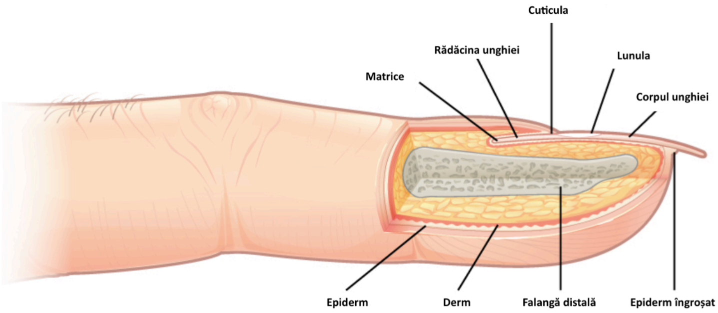

Figure 1.2 The anatomical structure of the human fingertip (University, Rice, 2018)

When considering the skin as a unitary whole incorporating its component elements, the epidermis, dermis and hypodermis, the skin can be classified as:

- anisotropic (Stark, 1977), (Gerhard, et al., 1981)
- viscoelastic (Pereira, et al., 1991)
- non-linear (Brown, 1973)
- non-homogeneous
- Properties that help take up large deformations.

Due to its viscoelastic properties, skin undergoes a phenomenon called preconditioning in which the relationship between stress and strain in loading-unloading cycles varies continuously until equilibrium is reached (Matsumura, et al., 2001), (Lui, et al., 2008). In-vivo skin is subjected to pre-stress (unit stress) present in variable magnitudes over the entire body surface at any time (Alexander, et al., 1977), (Jacquet, et al., 2008).

The mechanical response of the skin can be divided into 3 categories: (Brown, 1973)

Each phase of the given response has a counterpart in the behaviour of the collagen and elastin fibres in the dermis:

- Phase I illustrates high displacement at low forces;
- Phase II is related to collagen and elastin fibres that align in the direction of force application and increase the modulus of elasticity;
- Phase III - The fibres come under the direct influence of the force and the response is almost linear. (Brown, 1973)

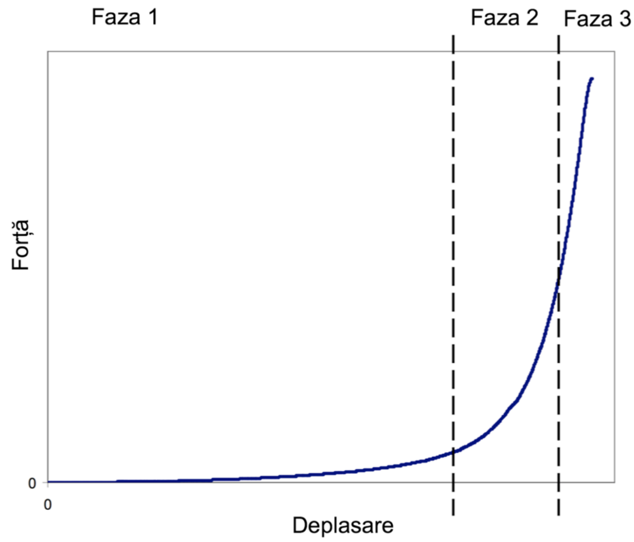

Figure 1.8 The mechanical response of the skin in vitro (Brown, 1973)

The in vivo examination method involves the evaluation of the mechanical properties of the skin under conditions closest to the natural state. As non-destructive methods for ethical reasons only 4 could be developed: torsion, tension, suction and punch indentation. Measured values of Young's modulus are presented in Table 1.2 below.

Table 1.2 In vivo measurements of Young's Modulus

Author	Young's Modulus	Location	Technique	Other data
(Bader, et al, 1983)	11,1-20 kPa	Arm/Leg	Indenter (20 mm)	
(Agache, et al, 1980)	0,42 MPa	Arm	Torsion (25 mm)	young skin
	0,85 MPa			old skin
	2,1 MPa	Back		stratum corenum
(Barel, et al, 1995)	0,13-0,17 MPa	Arm	Succion (2 mm)	
	0,20-0,32 MPa	Forehead		
(Diridollou, et al, 2020)	0,153 MPa	Arm	Succion (6 mm)	
(Sanders, 1973)	0,02-0,1 MPa	Arm	Torsion (8,7 mm)	
(Grahame, 1969)	18-57 MPa	Arm	Succion	
(Escoffier, et al, 1989)	1,1-1,32 MPa	Arm	Torsion	

Friction on the human skin is a complex phenomenon that cannot be described with the help of the classical theory of friction which can be summarised in the direct proportionality of the friction force with the normal force, described by Amontons and derived experimentally (Amontons, 1699).

The factors influencing friction behaviour are multiple. It is generally accepted that friction is influenced by the hydration level of the skin and the materials with which the skin is in contact. The consensus in many scientific papers is that an increase in surface roughness decreases the coefficient of friction and hydrophilic surfaces have a lower coefficient of friction than hydrophobic surfaces (Derler, et al., 2014); (Cua, et al., 1990); (Gerhardt, et al., 2008); (Adams, et al., 2007).

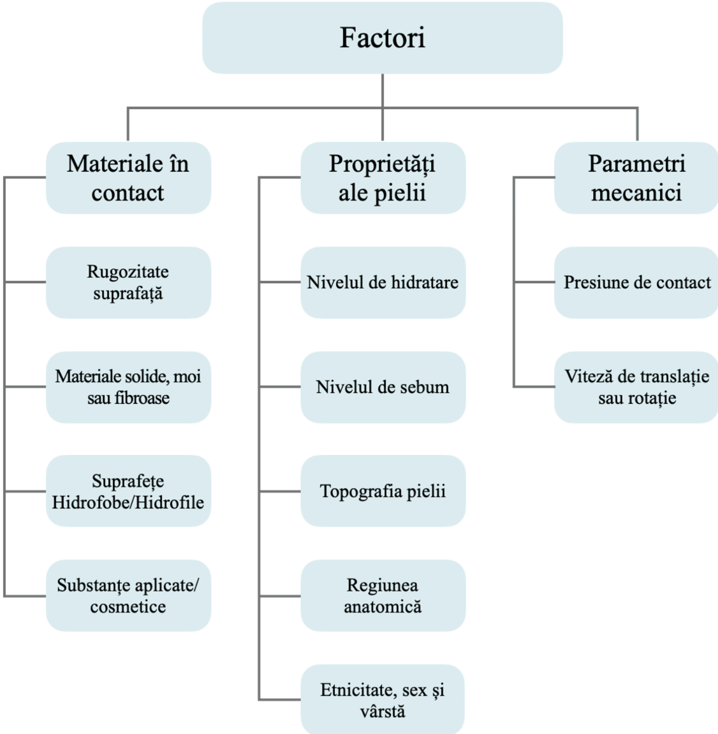

Figure 1.9 Factors influencing the friction behavior of human skin

Particularly for skin and skin friction, adhesion is a very complex phenomenon that is dependent not only on the level of hydration, roughness, possible treatments applied, the presence or absence of sebum, but also on other phenomena that occur between the two surfaces. (Goryacheva, et al., 2010), studied the influence of micro-geometry and adhesion interactions in viscoelastic bodies on contact and friction. The model used in their study was Maugis-Dugdale because the surface traction distribution is composed of two parts: the Hertz contact pressure and the Dugdale adhesion load (Johnson, et al., 1997).

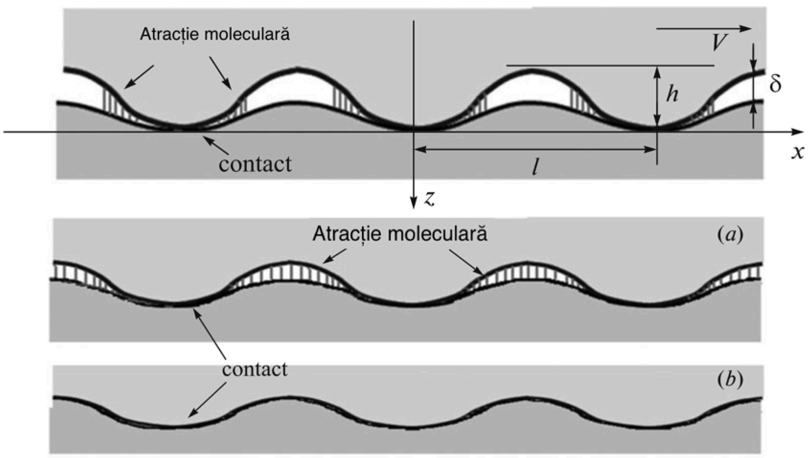

Figure 1.11 Types of contact studied by (Goryacheva, et al., 2010)

In Figure 1.11, we consider three different regimes: discrete contact in adhesive interaction regions, discrete contact in saturated adhesive interaction regions, and saturated contact. Depending on the characteristics of the interacting bodies and the loading conditions, one of these regimes (load and sliding speed) is achieved.

In **Chapter 2**, Theories used to model the state of stresses and strains in the contact of the human finger with artificial bodies, the different evaluation methods for the contact between solids are presented, simulations are performed to evaluate the non-conforming contact between solids with simple geometry, and two theoretical models are presented which describe the state of strains and stresses at the viscoelastic contact between the human finger and a rigid planar penetrator and the skin as an orthotropic material.

(Johnson, et al., 1971) describe how two solid bodies adhere and how the stresses and strains that occur as a result of contact between them can be described. Deformations are the result of two opposing forces and occur as a result of surface tension and elastic deformation.

The model was developed to describe the macroscopic character of the contact between a so-called soft solid and a rigid material but it was extended and applied to other material couples and on a smaller scale. The JKR model considers only the adhesion forces present on the contact area. The model is based on minimising the energy present in the deformation zone by balancing the adhesion energy favouring contact against the elastic energy opposing the deformations. Below, in Figure 2.14 you can see the difference between the Hertz contact area and the JKR contact area.

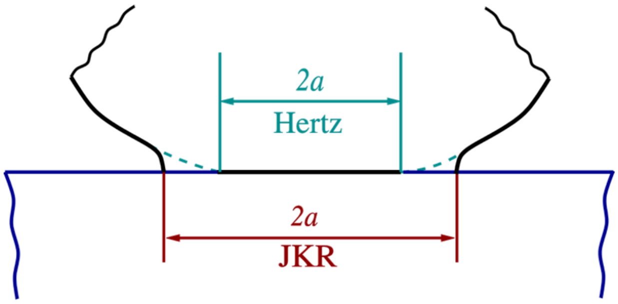

Figure 2.14 Contact area in the case of the JKR model relative to the Hertz model

For small bodies where the surface-to-volume ratio becomes significant or for soft materials, adhesive-type interaction forces must be included in the theoretical model. The DMT model developed by (Derjaguin, et al., 1975) folds on this type of contact and manages to faithfully describe the interaction between the bodies in contact. This model also includes interactions that occur outside the contact zone.

(Tabor, 1977) proposed a resolution of the contradiction between JKR and DMT theories. He presented a parameter called the Tabor Parameter, and showed that the two models are the extreme limits of a single parameterized theoretical model.

Models for the study of human skin can be composed of a structure similar to composite materials. An isotropic matrix incorporating one or more types of fibers with different mechanical properties can be used to generate the anisotropic mechanical properties of the skin. Using such a model can be a very good starting point when trying to simulate the mechanical character of soft tissues such as skin, as they can mimic the natural components of the tissue. Tissues such as muscles, ligaments, tendons, arteries, and skin are all made of a material that contains a matrix of fibers, thus allowing large deformations and anisotropic properties that differ depending on the orientation of the matrix and the fiber network.

To model the viscoelastic behavior of human skin, consider the case of a rigid rectangular penetrator in contact with human skin in the area of the fingers, Figure 2.16. The geometry of the punch is characterized by the length L and the width B which is much larger than the width b of the finger (B>>b). The skin and the respective tissue are fixed to the bone which is considered rigid (Soldatenkov, 2008). The rheological behavior of the skin can be approximated with the behavior of a Voight-Kelvin material. This material is characterized by its rigidities k_1 şi k_2 $\left(\frac{Pa}{m}\right)$ and the local viscosity parameter η $\left(\frac{Pa \times s}{m}\right)$.

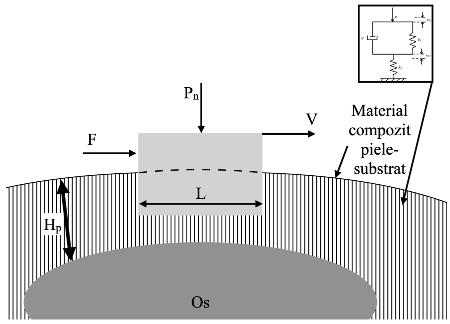

Figure 2.16 Schematisation of contact finger-rectangular plane

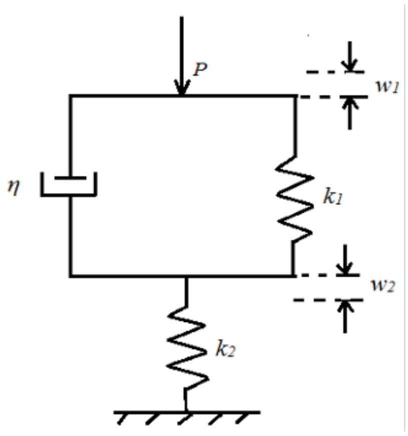

Figure 2.17 Rheological model of human skin (Voigt-Kelvin type material)

Voigt-Kelvin material constitutive equation at point ξ on the contact surface, characterised by pressure p_ξ, can be expressed as: (Cheng et al., 1999, Soldatenkov 2008)

$$\eta \frac{\mathrm{d}}{\mathrm{d}t} u_{1\xi} = k_1 u_{1\xi}(t) = p_\xi(t); \; k_2 u_{2\xi}(t) = p_\xi(t)$$ Ecuation 2.57

where $u_{1\xi}$ şi $u_{2\xi}$ are the displacements at a point ξ from the viscoelastic zone of viscosity η and rigidity k_1 and from the rigidity zone k_2, t is the time, p_ξ is the contact pressure at point ξ.

For the flat penetrator:

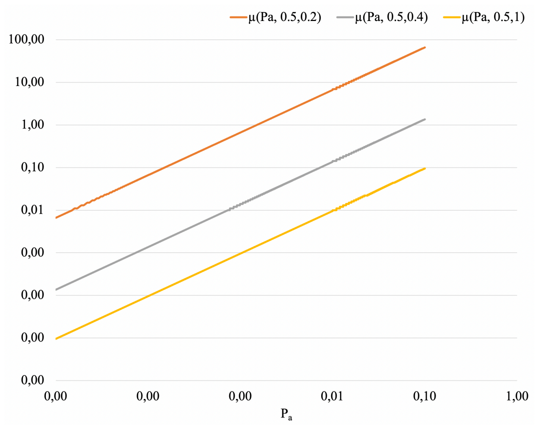

Figure 2.18 The variation of the deformation component of the friction coefficient with the dimensionless load and different dimensionless speeds

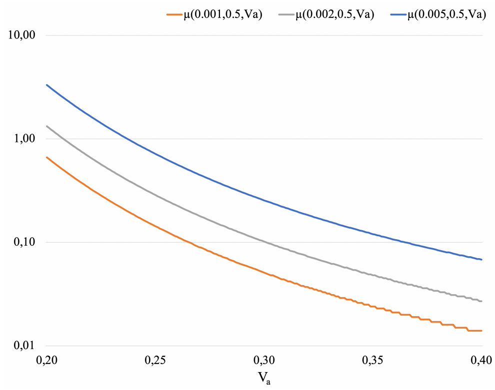

Figura 2.19 Variation of the deformation component of the friction coefficient with the dimensionless velocity and different dimensionless loads

Figure 2.19 shows the decrease in the deformation component of the friction coefficient when the sliding speed increases, which represents a condition for the occurrence of the stick-slip phenomenon.

Figure 2.20, below, exemplifies the dimensionless pressure variation between the finger and the straight-edged planar penetrator along the contact length.

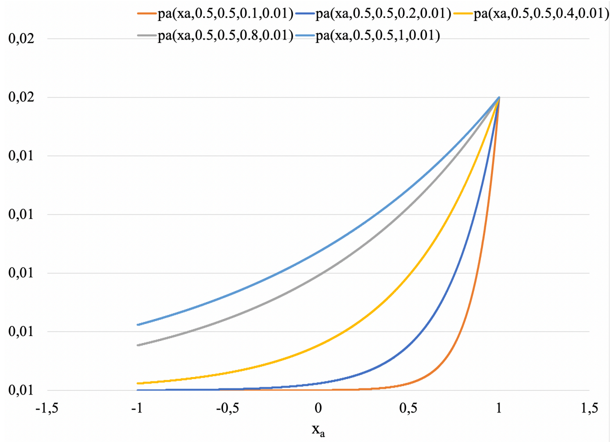

Figure 2.20 Variation of pressure along the contact length for different dimensionless velocities v_a

It can be observed that at the entrance of the contact, the pressure is maximum and is a function of the relative penetration.

The case of the punch with the plane profile connected to the ends with parabolas:

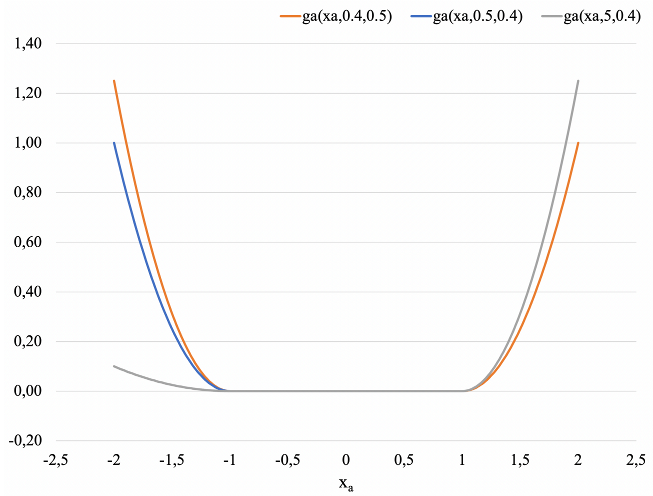

Figure 2.21 Flat penetrator connected parabolically at the ends

Figure 2.22 exemplifies the pressure distribution on the planar punch connected parabolically at both ends.

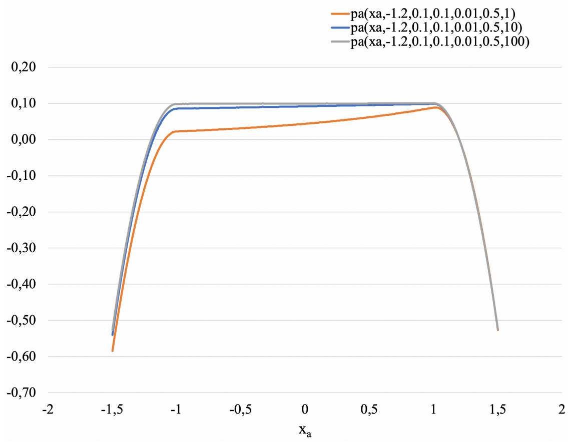

Figure 2.22 Pressure distribution on the planar penetrator connected parabolically at both ends

The effect of the sliding speed between the punch and the finger on the pressure in the center of contact is shown in Figure 2.22.

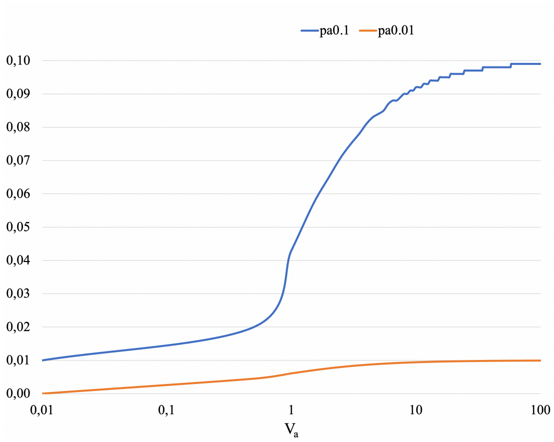

Figura 2.23 Variația presiunii din origine funcție de viteza de alunecare

Figure 2.30 shows the pressure variation *p* on the mobile punch for different speeds, penetrations and connection radii.

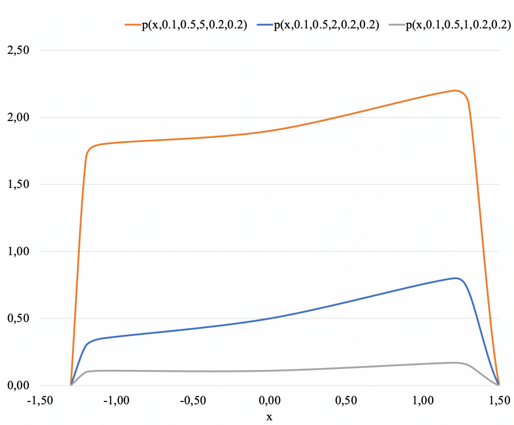

(a)

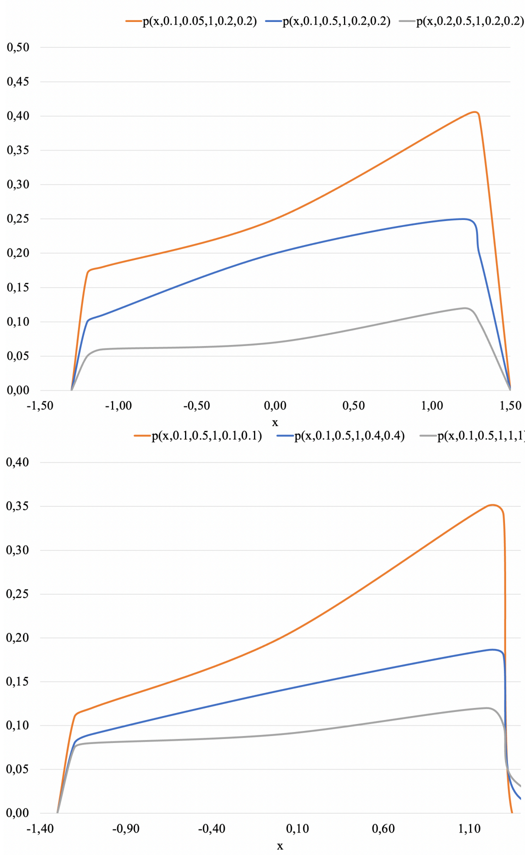

(b)

(c)

Figure 2.30 Variation of contact pressure on the parabolically connected punch at the ends for different speeds (a), penetrations (b) and symmetrical connection radii (c)

An important parameter for the condition of the contact between the finger and the flat punch is the sliding speed. Figure 2.31 exemplifies the pressure variation in the center of the punch at v_u, for different penetrations.

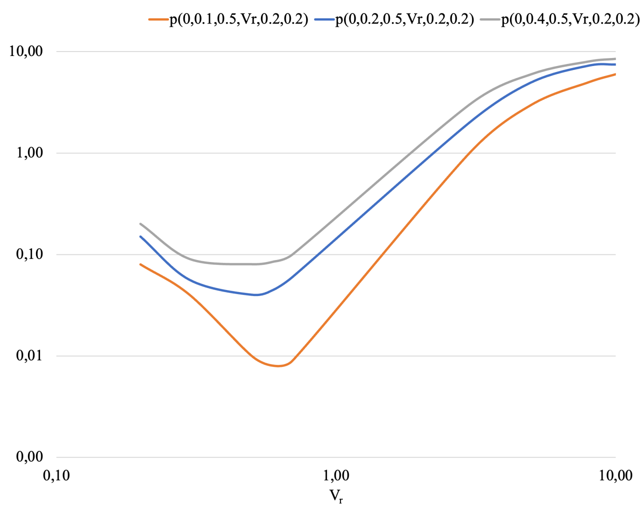

Figure 2.31 Variation of contact pressure at the center of the punch with sliding speed

A model for the anisotropy of human skin that considers four directions is presented below. The viscoelastic skin model with orthotropic anisotropic behaviour is considered. This model allows the determination of viscoelastic characteristics in any direction if these characteristics are known along four directions: at 0°, at 45°, 90° and at 135°. The calculation model is adapted from (Khatyr et al. 2004).

The total deformation can be exemplified:

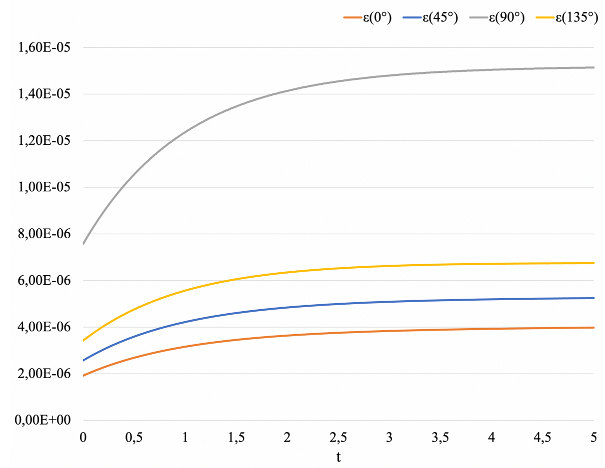

Figure 2.33 Total deformation ε for different angles

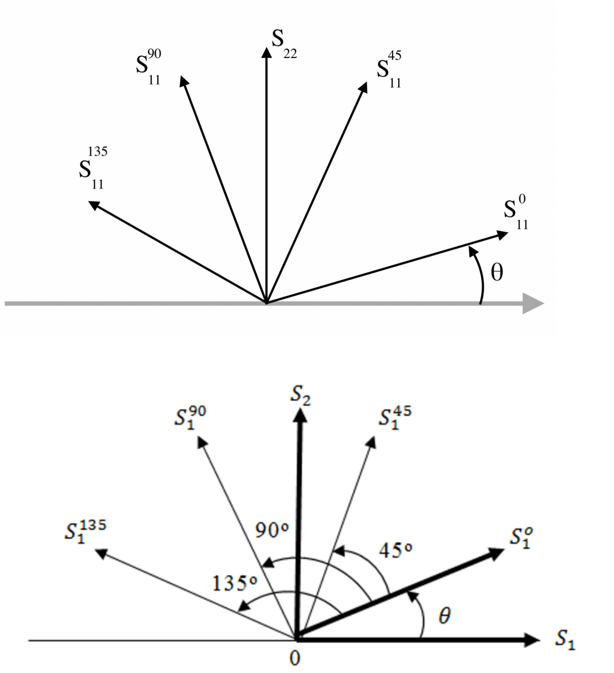

Figure 2.34 Directions of evaluation

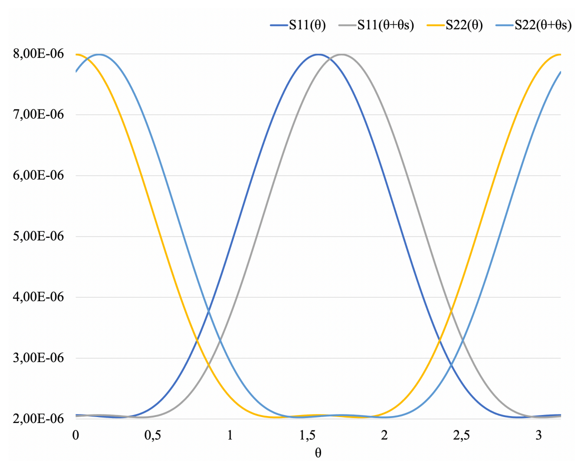

Figure 2.35 Variation of flexibility coefficients with random angle, θ

Chapter 3 assesses the shape and size of the fingers in combination with skin topography as among the most important factors contributing to the mechanical response of hand-to-object contacts. The purpose of this chapter is to describe the shape and geometry of the human finger.

Table 3.1 Table of average sizes grouped by gender (mm)

Finger	Sex	Length (mm)	Standard deviation	Width (a)	Standard deviation	Thickness (b)	Standard deviation	Circumference (mm)
Thumb	M	61,98	1,86	24,45	1,38	14,37	2,35	124,02
	F	57,94	5,81	20,08	2,26	12,45	1,62	103,60
Index	M	90,45	2,79	19,03	1,78	12,36	2,18	99,74
	F	79,47	1,74	16,38	1,44	10,90	1,85	86,56
Middle finger	M	101,73	3,25	20,72	2,13	13,46	2,44	108,60
	F	85,21	1,70	17,61	1,54	11,72	1,91	93,06
Ring finger	M	93,35	3,07	17,50	1,56	12,62	2,72	95,24
	F	83,62	2,03	14,96	1,07	9,33	1,19	77,35
Small finger	M	74,01	2,25	16,09	1,71	10,86	1,71	85,45
	F	63,27	1,83	14,86	1,07	7,79	2,06	72,92
Palm	M	110,87	4,42	92,45	2,73	-	-	-
	F	94,77	3,86	84,20	2,66	-	-	-
Hand	M	199,15	6,52	-	-	-	-	-
	F	172,89	4,77	-	-	-	-	-

Figure 3.4 below shows how the contact area measurement was performed. It can be seen how the actual contact area increases in direct proportion to the applied force.

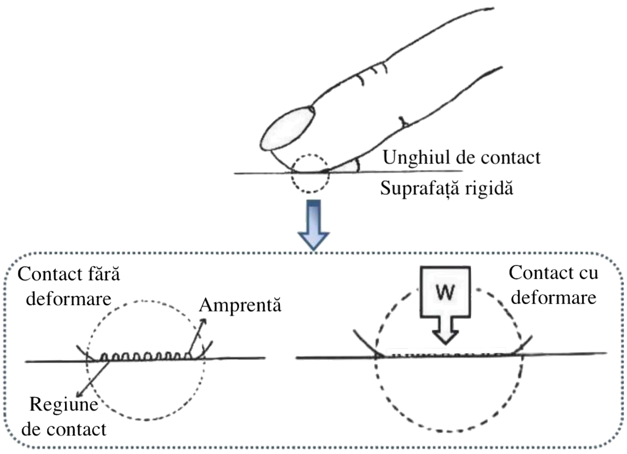

Figure 3.4 Variation of contact area with applied force

Table 3.2 Experimental measurements of the contact area between fingers and a rigid surface

Deget	Sex	Average contact area (mm²)
Finger	M	292
Thumb	F	274
	M	143
Index	F	1,26
	M	190
Middle finger	F	165
	M	175
Ring finger	F	160
	M	130
Small finger	F	115

Due to the need to have a model as close as possible to reality in order to perform complex simulations of the behaviour of the human finger and skin, a 3D scan of an index finger was performed.

Figure 3.5 STL model of a finger

The model was processed using Autodesk Fusion 360 Ultimate software. Thus, a solid type study model was generated with 104759 TET10 type elements and 152529 nodes.

Figure 3.6 Solid study model

Since the articulation of the phalanges of the fingers was not relevant to the subject of the simulations, a continuous rigid support was chosen to respect the thickness of the tissue covering the bony support of a real finger. This can be seen in Figure 3.15 below.

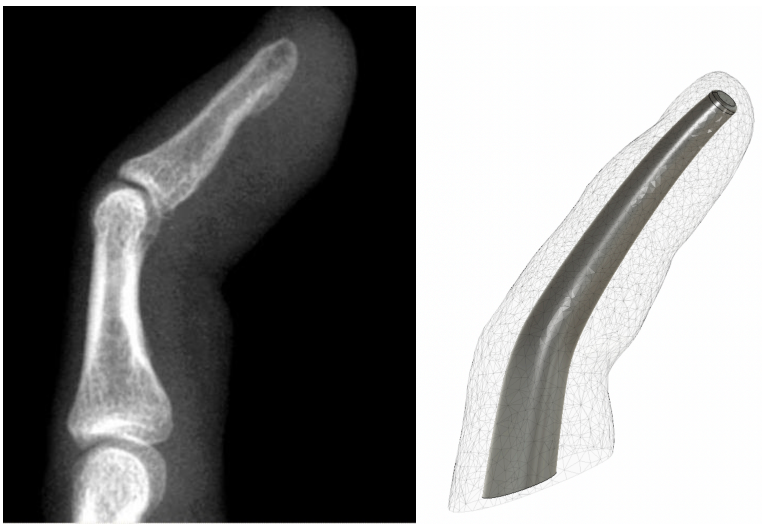

Figure 3.15 X-ray of a human finger and model for the rigid support

Below, in figure 3.17, you can see the state of deformations at the level of the skin substrate in the case of indentation with a spherical type penetrator.

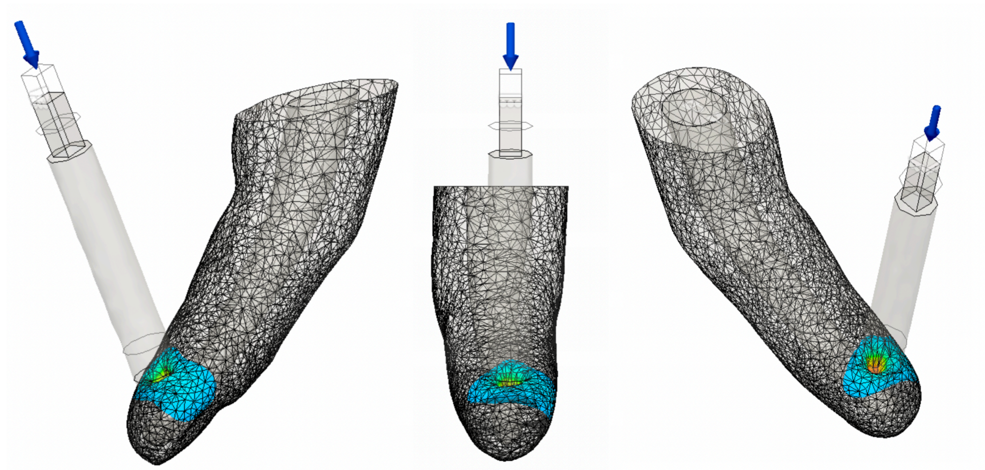

Figure 3.17 State of deformations obtained for the case of punch with diameter 8 mm and force 5 N

Chapter 4 presents experimental studies to determine the friction parameters between human finger skin and various artificial surfaces and to determine the material characteristics of the skin and substrate.

The stick-slip phenomenon refers to the vibration that occurs when the coefficient of static friction is greater than the coefficient of kinetic friction in the case of relative displacements of two solids in contact. The term stick-slip is derived from the English language, "stick"-sticking "slip"-sliding. The phenomenon of stick-slip or friction-induced vibration is a phenomenon that occurs at low and very low speeds. The effect is mostly undesirable, as the vibrations produced can damage mechanical systems or disturb acoustics through high-intensity and high-frequency noises, but it can also be desired in the case of bowed musical instruments such as the violin. The phenomenon is present in the case of automobile brakes, clutches, and is a generator of positioning errors in the case of machine tools.

The stick slip phenomenon appears, therefore, if the relative speed v_r is lower than the value of the speed for which the slip is stable, and it also depends on the stiffness characteristics of the system and the friction behaviour of the two materials in contact (Baumberger, 1995) , (Popov, 2010), (Wensrich, 2006). The stick-slip motion is conditioned by the ratio of the coefficient of static friction μ_s to the coefficient of kinetic friction μ_k and occurs only when the ratio is above unity (Gao, et al., 1994), (Gao, et al., 1993).

From the work of (Baumberger, 1995) it can be seen, in Figure 4.4, how the coefficient of friction varies with speed.

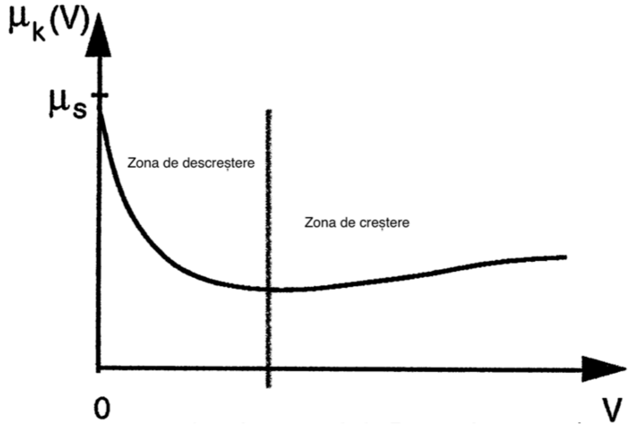

Figure 4.4 Dry friction at low speeds(Baumberger, 1995)

Experiments were carried out on the "Stick-Slip" stand of the Department of Machine Elements and Tribology. Below, in Figure 4.6, the stand can be seen, presented schematically, and the component elements of the stand can be observed, together with the adaptation brought to be able to perform measurements on the fingers.

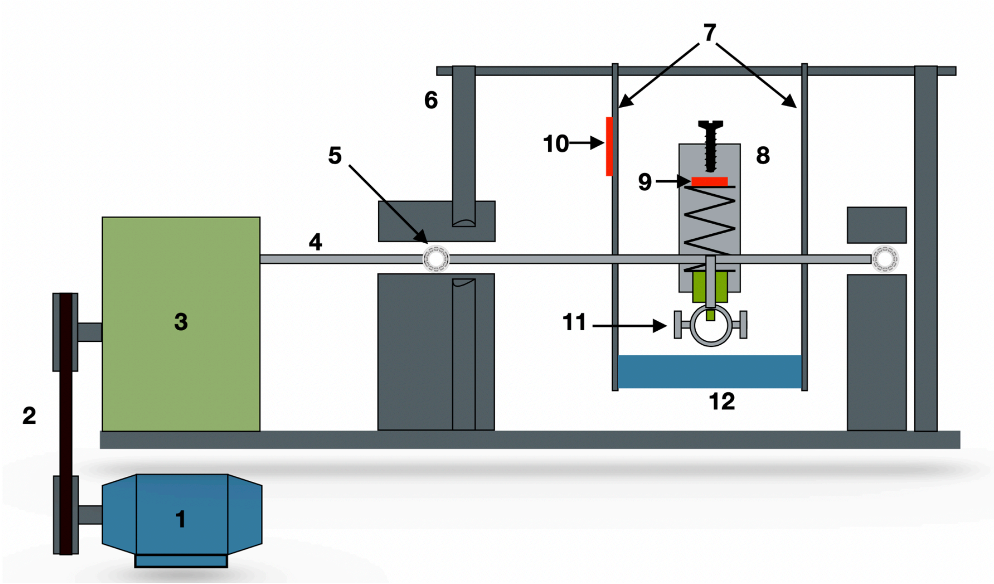

Figure 4.6 Schematic model of the experimental stand

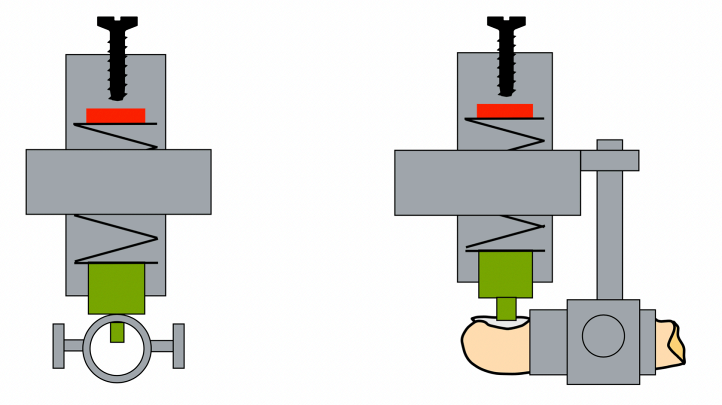

Figure 4.7 Schematic model for the finger immobiliser

To stiffen the joints and immobilise the finger, an aluminum tube was used and the space between the tube and the finger was filled with plaster. This can be seen in Figure 4.8 below.

Figure 4.8 Finger stiffening method

The materials tested were steel, bronze and 3 types of materials found on the inside of work gloves that are in direct contact with human skin: leather (bovine origin) and 2 types of textiles (cotton and nylon). The materials were surface evaluated using the Surtronic 25 Surface Roughness Tester profilometer manufactured by Taylor Hobson Ltd, with a resolution of Ra 0.01

µm - Rz, 0.1 µm and an accuracy of 2%. The probe tip is a diamond with a tip radius of 5 µm. The digital filter for signal processing is Gaussian (ISO 11562). Below, in Figure 4.10, you can see both the types of materials and the direction and meaning on which the measurements were made.

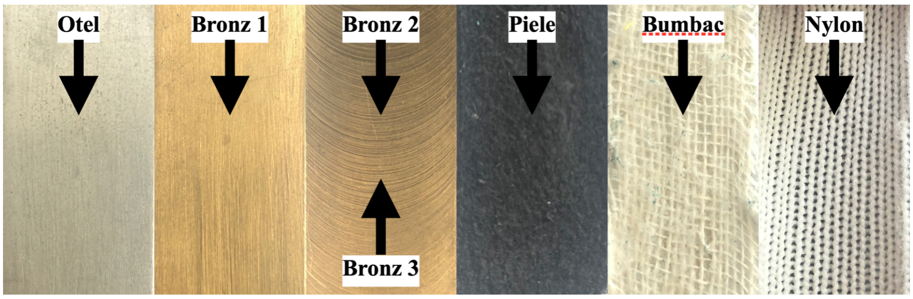

Figure 4.10 The material samples used in the evaluation of the coefficient of friction, indicating the direction and meaning of the measurements

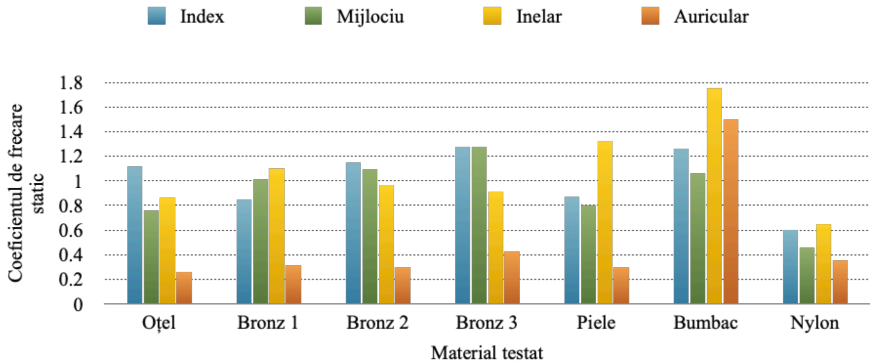

Figure 4.11 The coefficient of static friction relative to the tested material for each finger

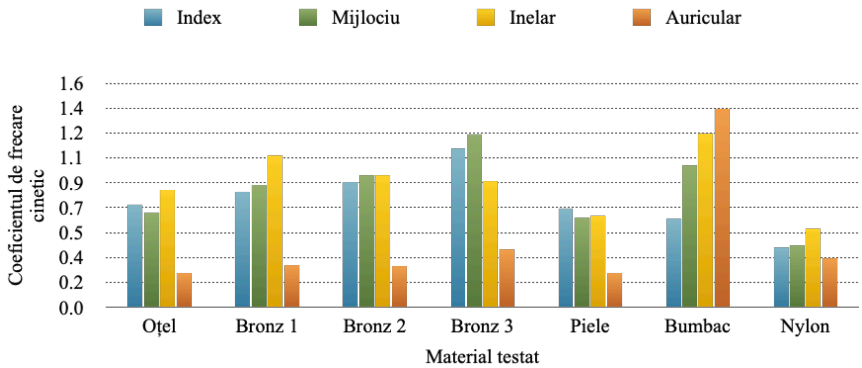

Figure 4.12 The coefficient of kinetic friction relative to the tested material for each finger

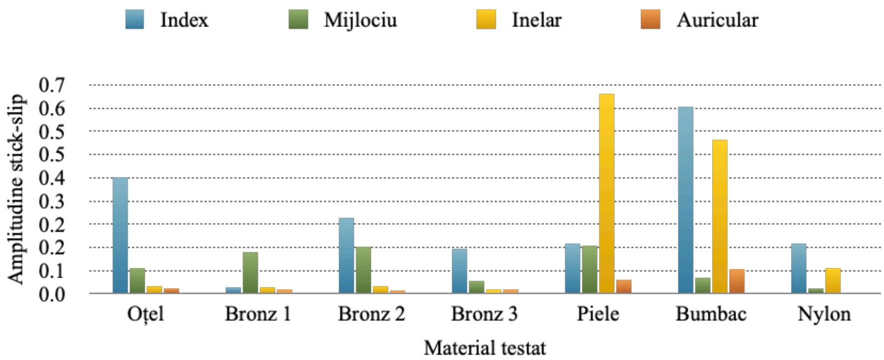

Figure 4.13 Amplitude of the stick-slip phenomena

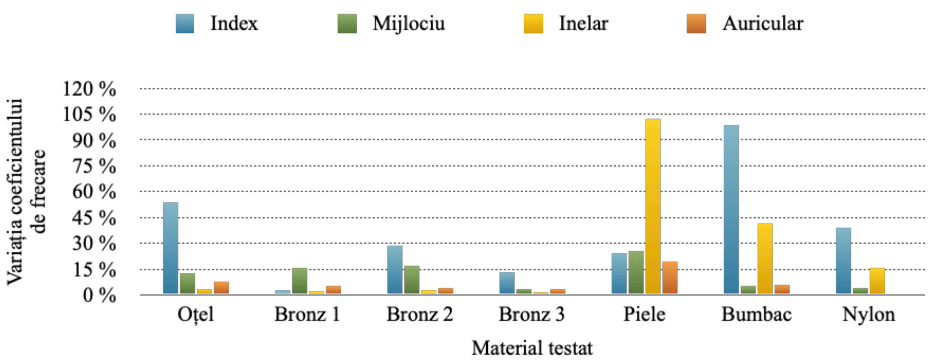

Figure 4.14 Variation of the static friction coefficient

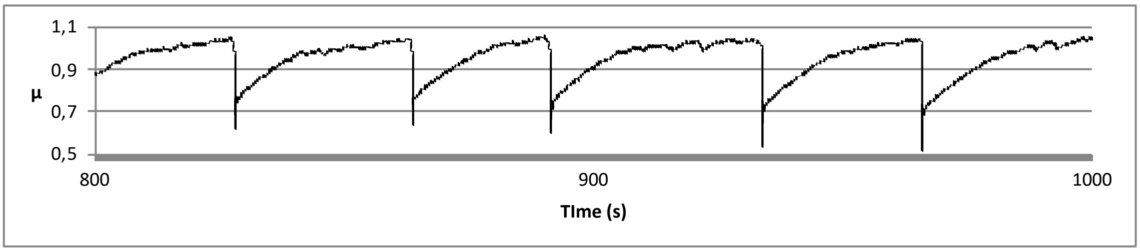

Figure 4.15 Index - Coefficient of friction for steel

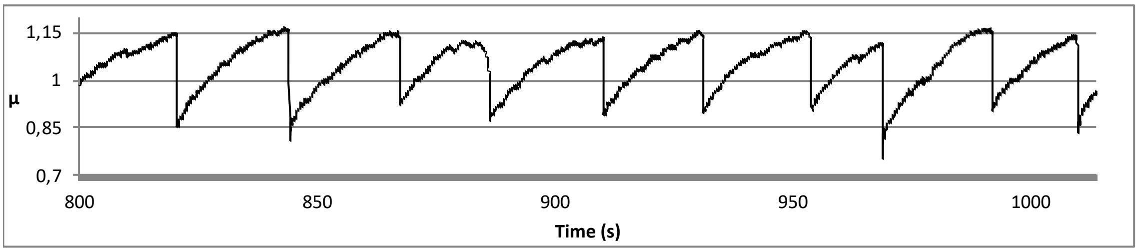

Figure 4.24 Middle finger - Coefficient of friction for bronze 2

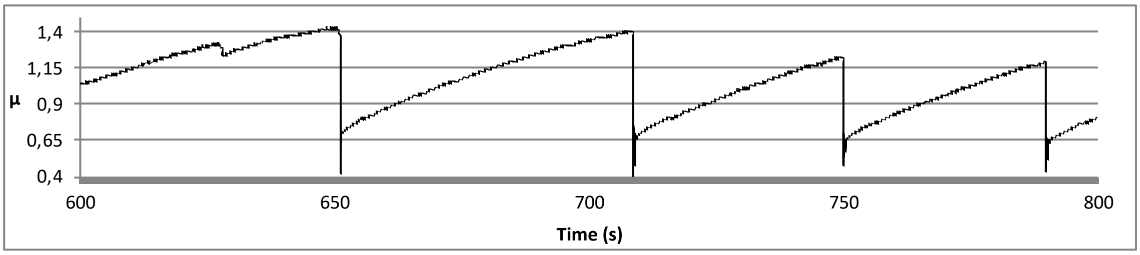

Figure 4.33 Ring finger - Coefficient of friction for leather

The experimental models were also developed for the CETR (currently Bruker) UMT-2 stand, a stand that allows the evaluation of the friction force at very low speeds.

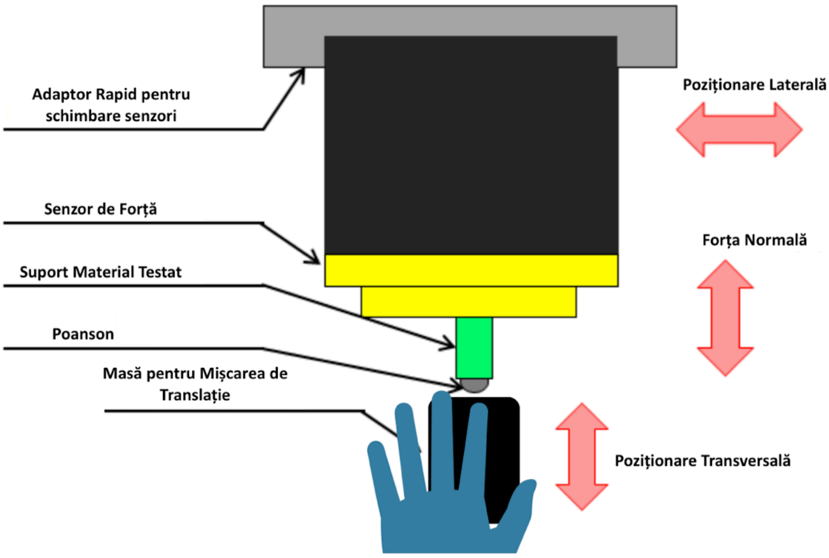

Figure 4.43 Schematic representation of the UMT-2 tribometer

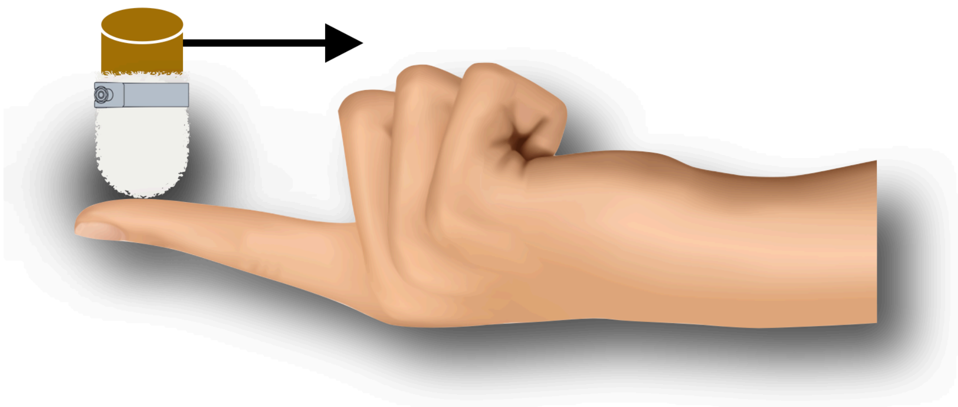

Figure 4.44 Schematic representation of the experiment

The most important observation that emerges from the experiments performed is the identification of a so-called creep friction coefficient, which is directly determined by the flattening phase of the stick-slip curve.

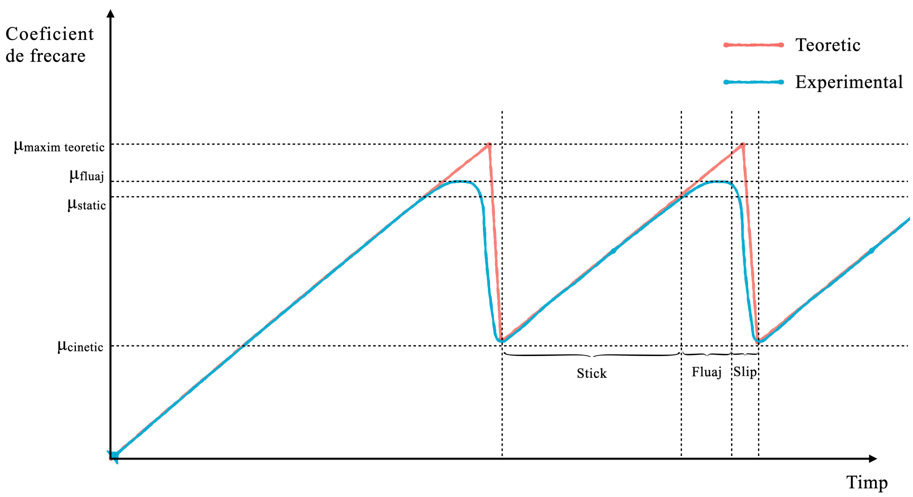

Figure 4.46 Diagram for determining friction coefficients

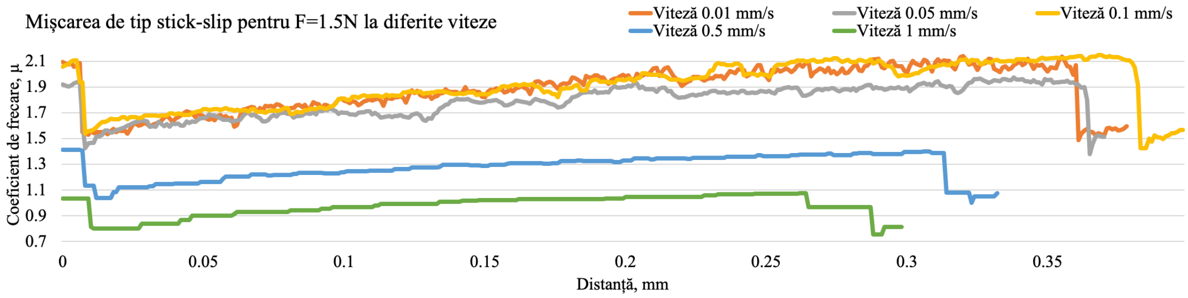

Figure 4.47 Comparison of the distance traveled for a stick-slip cycle for a force of 1.5 N

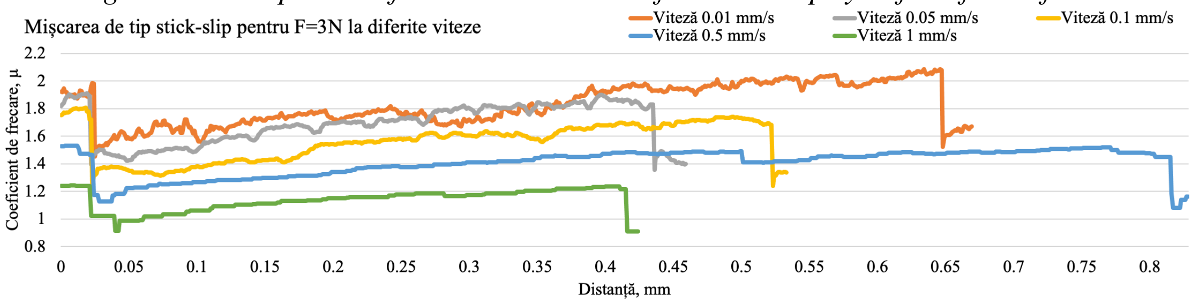

Figure 4.48 Comparison of the distance traveled for a stick-slip cycle for a force of 3 N

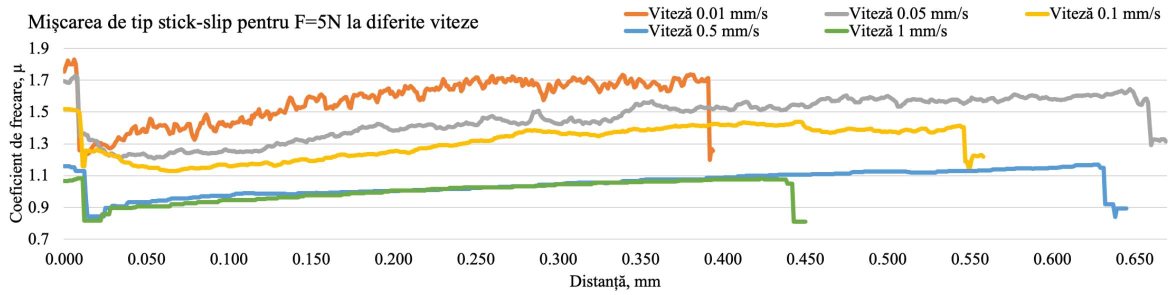

Figure 4.49 Comparison of the distance traveled for a stick-slip cycle for a force of 5 N

The creep phenomenon can be categorised as a precursor of slip (microslip) with energy release several orders of magnitude smaller than the major slip event. This phenomenon can be seen very clearly in the inconstancy of the increase of the coefficient of friction at low and very low speeds. Below, Figures 4.49-4.54 highlight the microslip zones that are present in the context of a stick-slip cycle for all forces at all speeds. Microslip zones occurring at speeds of 0.01 mm/s and 0.1 mm/s were exposed, but this character of stick-slip motion occurs at all speeds tested.

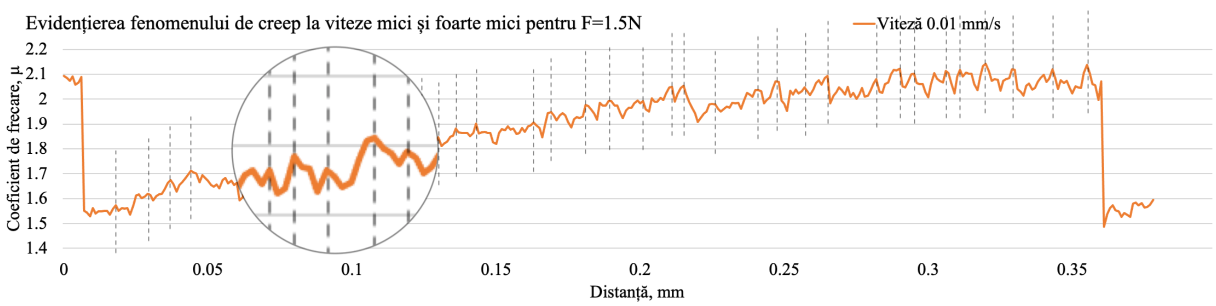

Figure 4.50 Highlighting the creep phenomenon at F=1.5N and v=0.01 mm/s

To determine the contact area between the finger and a rigid punch, the CETR-UMT2 experimental stand was used. The contact area was determined using three punches made of cylindrical bronze with sphere termination with diameters of 8 mm, 12 mm and 28 mm at three different forces (1.5 N, 3 N and 5 N).

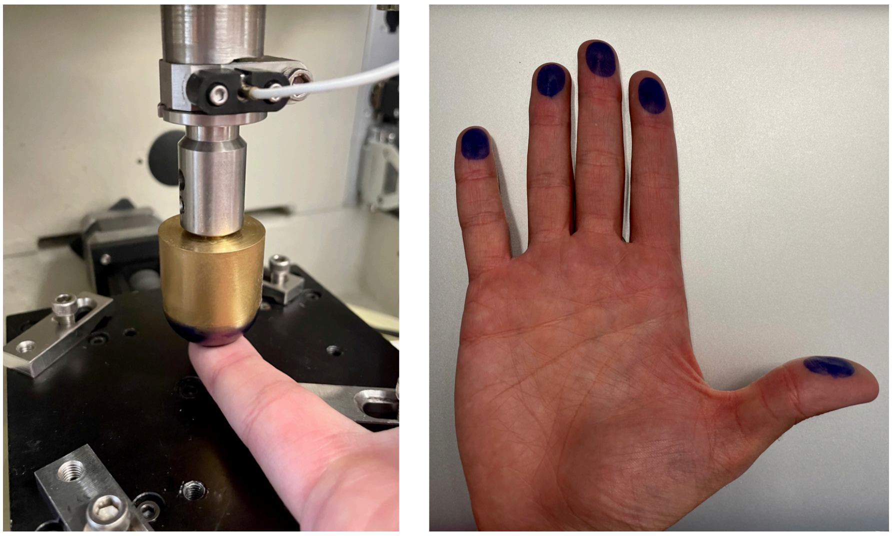

Figure 4.59 Measuring contact area with a rigid punch

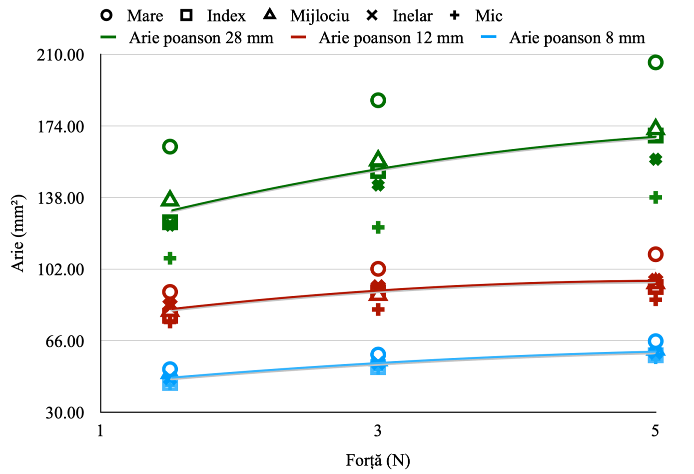

Figure 4.60 Contact area determined for human fingers

Before developing a theoretical model to describe a tissue it is beneficial to determine the general mechanical properties of that tissue. Due to the fibers within the tissue tending to have preferred directions, depending on the part of the body on which the experiments are performed, soft tissues have a predominantly anisotropic behavior. Thus, indentation creep measurement on the "CETR-UMT2" stand and determination of Young's modulus for human finger skin was performed and Young's modulus for human finger skin was determined.

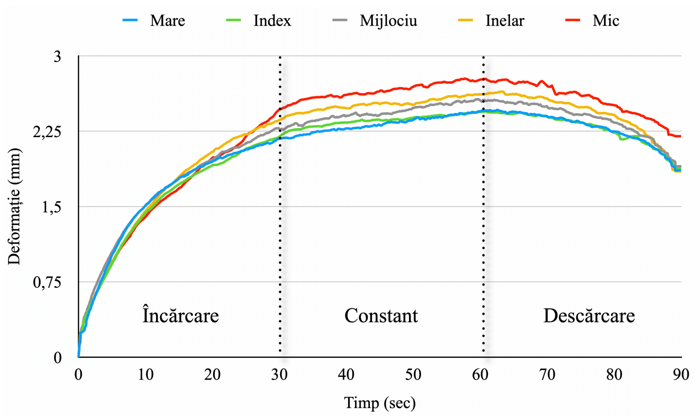

Figure 4.69 Complete Cycle — 8mm indender, 3N force

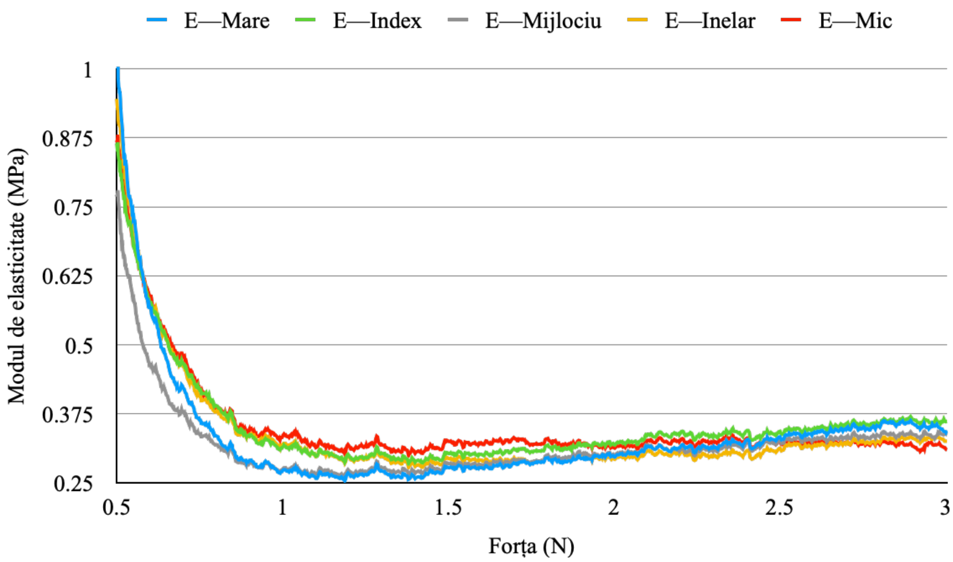

Figure 4.71 The modulus of elasticity calculated for the skin of human fingers — punch 8mm

Chapter 5 presents the theoretical modeling of the stick-slip phenomenon with the inclusion of creep and contact stability. The theoretical model developed is based on the theoretical model proposed by (Nakano and Maegawa, 2009a), a model that has only one degree of freedom. A law of logarithmic dependence between the friction coefficient and stick time and drive speed can be deduced from the experiments.

$$\mu_s = a_s + b_s \ln\left(\frac{\tau}{\tau_0}\right) = c_s + b_s \ln\left(\frac{D_0}{\tau}\right)$$ Ecuation 5.1

$$c_s = a_s - b_s \ln\left(\frac{\tau_0}{D_0}\right)$$ Ecuation 5.2

Where:

a_s și b_s are factors of the logarithmic equation;

$\frac{\tau}{\tau_0}$ represents the non-dimensionalisation of the stick time;

D_0 is a specific length to normalise the curves for the kinetic part and the static part on a double logarithmic scale.

Analogously, the kinetic friction coefficient can be expressed in the form:

$$\mu_k = a_k - b_k \ln\left(\frac{v}{v_0}\right) = a_k - b_k x_v$$ Ecuation 5.3

In the experiments presented in the previous chapter, this friction coefficient has the value of the kinetic friction coefficient at the end of the slip period.

Stick, slip-I and slip-II are the three different types of friction states. There are two types of friction, static friction F_s and kinetic friction F_k.. The condition of friction is determined by the relative speed between the surfaces in contact:

$$\mu = \begin{cases} F_s \, if \, V - \dot{x} = 0 : stick \\ F_k \, if \, V - \dot{x} > 0 : slip\ I \\ -F_k \, if \, V - \dot{x} < 0 : slip\ II \end{cases}$$ Ecuația 5.9

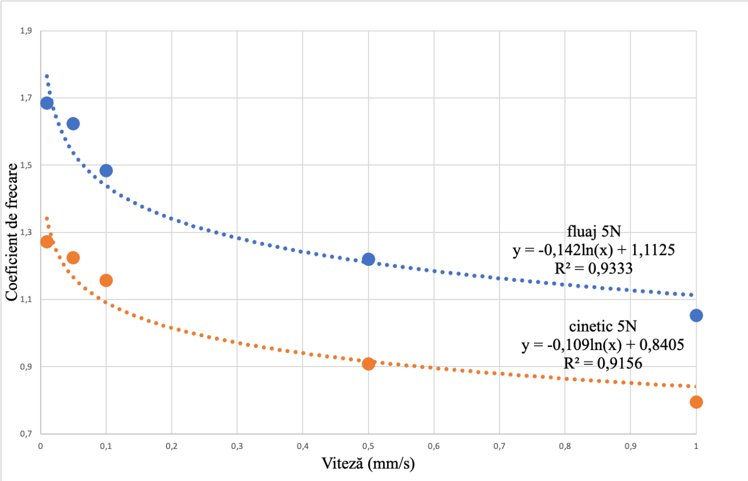

Figure 5.1 Kinetic friction and creep coefficients on a logarithmic scale for F=5N

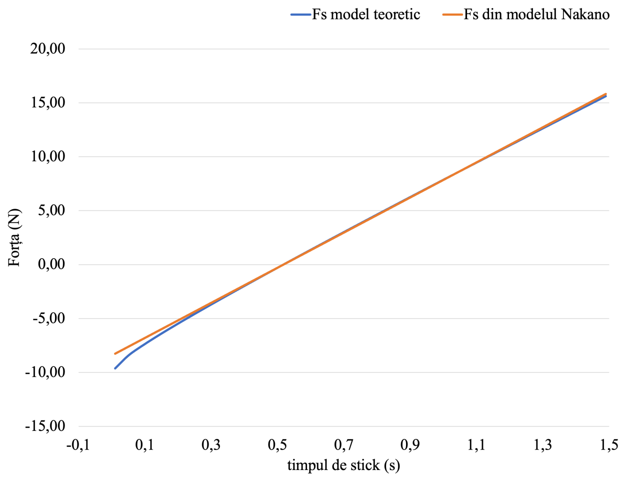

Figure 5.6 The similarity between the theoretical model developed and the model developed by (Nakano and Maegawa, 2009a)

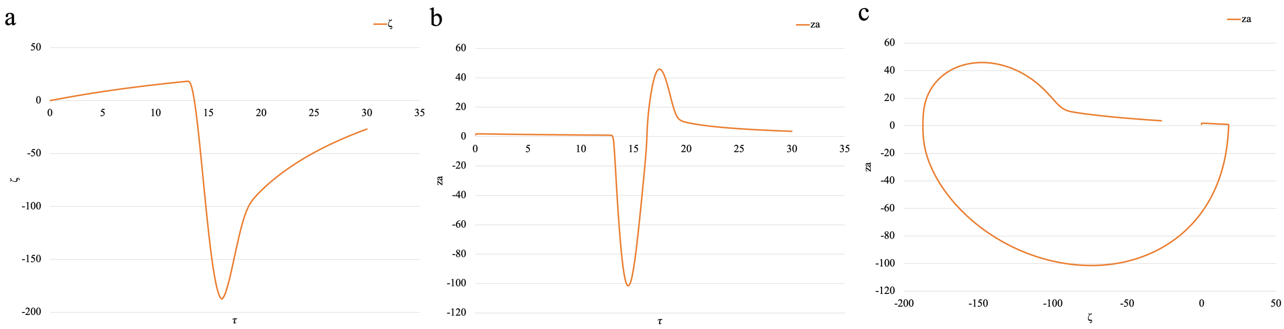

Figure 5.10 (a,b,c) Numerical solution of dimensionless parameters ξ, z_a and τ for $\xi' < 1$

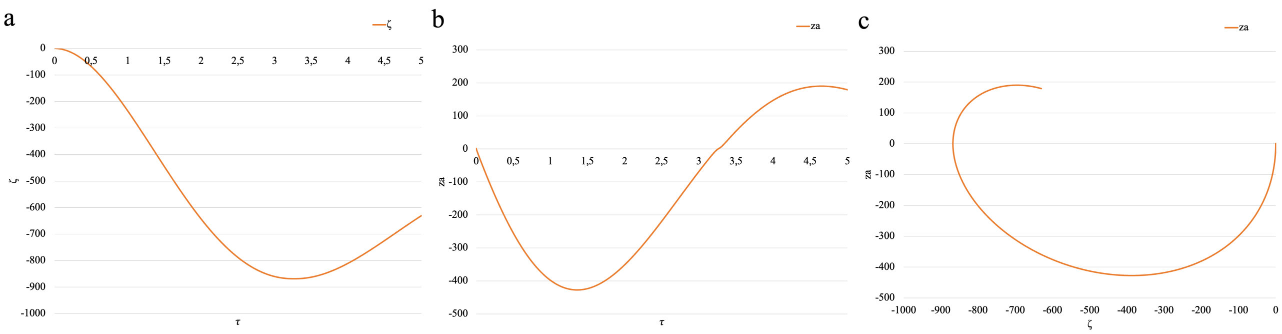

Figure 5.11 (a,b,c) Numerical solution of dimensionless parameters ξ, z_a and τ for $\xi' > 1$

To determine the dynamics of a system with friction, taking into account the discontinuity between static and kinetic friction and the dependence of the coefficient of kinetic friction on the relative velocity, the logarithmic friction law used in the presented system depends on five dimensionless parameters $(\lambda, \zeta, \gamma, \Delta\lambda, \alpha)$.

The stick-slip phenomenon certainly occurs in a system with friction without viscous damping. The stick-slip boundary is produced by viscous damping, which is controlled by the stick-slip parameter (λ) and the damping parameter (ζ), two dimensionless parameters.

Experimentally, the dependence of the static friction coefficient, μ_s, and the kinetic friction coefficient, μ_k, on the stick time, velocity and normal force was observed, and the developed model takes these dependencies into account in the friction dynamics.

GENERAL CONCLUSIONS

- Tribological phenomena between the skin of human fingers and man-made objects are essential for grasping and manipulating objects. The transmission of forces and moments through the contact of the fingers with various objects is done by both form and static friction.
- In order to know the skin-finger-object interface aspects, it is necessary to determine the contact pressure, local deformation, relative velocity and static and kinetic friction coefficients.
- The skin of human fingers has a viscoelastic behavior of the Hooke-Voigt-Kelvin type and can be characterized by elastic, elastoplastic deformations and after a long time (on the order of seconds and tens of seconds), the skin is characterized by a Voigt-Kelvin type spectrum.
- The essential tribological parameters (contact pressure, deformation, coefficient of friction) of the contact of human fingers with different objects depend on the speed, in the case of relative movement, and the duration of the grip, in the case of objects that can be fixed in the hand by means of the fingers.
- At relatively low velocities, the case of initiation of attachment or detachment of objects, the stick-slip phenomenon occurs.

CONTRIBUTIONS

The doctoral thesis makes the following contributions:

1. Literature review

- Study on the evolution of works in the field of biotribology;
- Bibliographic synthesis on the tribology of human skin;

2. Experimental study

- Determining the geometry of human fingers by adapting a 3D scanner and validating the model by comparing the results obtained from simulations with experimental ones;
- Adaptation and modification of the devices of the "Stick-slip" and CETR-UMT2 experimental stands for the study of finger friction with various synthetic materials;
- Highlighting the appearance of the creep phenomenon at the end of the stick phase and at the beginning of the slip phase;
- Determination of static and kinetic friction coefficients between finger skin and various synthetic materials and detection of logarithmic dependence on contact pressure and speed;

- Determination of the contact area between the tip of the finger and rigid surfaces;
- Experimental highlighting of the dependence of the static friction coefficient on the stationary time;
- Determination of the elasticity parameters of the skin of the fingers from penetration tests;

3. On a theoretical level and modelling

- Theoretical models and calculation programs in MATCHAD 14, regarding the state of stresses and deformations during the viscoelastic contact of human fingers with:
  - a rigid plane with straight and rounded parabolic edges;
  - a cylinder;
  - a sphere;
- Theoretical models designed include dimensionless parameters and can be used as similarity criteria.
- Adaptation of a theoretical model regarding the anisotropy of the skin of human fingers and the creation of a calculation program.
- Theoretical model and calculation program regarding the stick-slip phenomenon at the contact of the human finger with different rigid flat surfaces by taking into account the evolution of the friction coefficients and the additional creep phase (stick-creep-slip).
- Theoretical model and calculation program on the stability of finger movement on rigid surfaces at low and very low sliding speeds.

4. Perspectives

- Effects of sweat and normal water on the tribological parameters of human finger skin;
- Optimisation of the surface texture in order to increase the coefficient of static friction for artificial leather.
- Comparison of the tribological parameters of human skin with artificial skin in order to optimise the gripping surfaces of different objects by robots.
- Development of a finite element model incorporating more details and more experimentally determined parameters.

Selective Bibliography

1 **Adams, M, Briscoe, B și Johnson, S. 2007.** *Friction and lubrication of human skin*. s.l. : Tribology Letters, 2007. pg. 239-253. Vol. 26(3).

3 **Agache, P și Humbert, P. 2004.** *Measuring the Skin—Non-Invasive Investigations*. Berlin : Physiology, Normal Constants, 2004. Vol. 1.

5 **Agache, P, și alții. 1980.** *Mechanical properties and Young's Modulus of human skin in vivo*. s.l. : Archives of Dermatological Research, 1980. pg. 221-232. Vol. 269.

7 **Alexander, H și Cook, T H. 1977.** *Accounting for natural tension în mechanical testing of human-skin*. s.l. : Journal of Investigative Dermatology, 1977. pg. 310-314. Vol. 69.

8 **Amontons, G. 1699.** *De la re´sistance cause´e dans les machines*. Paris : Mémoires de l'Académie royale des sciences, 1699. pg. 257-282. Vol. A12.

16 **Bader, D și Bowker, P. 1983.** *Mechanical characteristics of skin and underlying tissues in-vivo*. s.l. : Biomaterials, 1983. pg. 305-308. Vol. 4.

17 **Barel, A O, Courage, W și Clarys, P. 1995.** *Suction method for measurement of skin mechanical: the Cutometer.* s.l. : Handbook of Non-Invasive Methods and the skin. Boca Raton, CRC Press, 1995. pg. 335-340.

19 **Baumberger, T. 1995.** *Dry friction Dynamics at low velocities*. s.l. : Physics of Sliding Friction, Springer, 1995.

28 **Brown, I A. 1973.** *Scanning electron-microscope study of effects of uniaxial tension on human skin*. s.l. : British Journal of Dermatology, 1973. pg. 383-393. Vol. 89.

32 **Cheng, L, Xia, X, Yu, W, Scriven. L E, Gerberich, W W.** *1999, Flat-Punch Indentation of Viscoelastic Material. Journal of Polymer Science: Part B: Polymer Physics, Vol. 38, 10–22 (2000) © 2000 John Wiley & Sons, Inc.*

39 **Cua, A B, Wilhelm, K P și Maibach, H I. 1990.** *Frictional properties of human skin: relation to age, sex and anatomical region, stratum corneum hydration and transepidermal water loss*. s.l. : British Journal of Dermatology, 1990. Vol. 123(4).

41 **Dawson, D și Wright, V. 1973.** *Bio-tribology, in: Proceeding of the Conference on the Rheology of Lubrication*. London : The Institute of Petroleum, The Institution of Mechanical Engineers, and the British Society of Rheology, 1973. pg. 81-88.

47 **Derjaguin, B V, Muller, V M și Toporov, Y P. 1975.** *Effect of contact deformations on the adhesion of particles*. s.l. : Journal of Colloid and Interface Science, 1975. pg. 314-326. Vol. 52(2).

49 **Derler, S, și alții. 2014.** *Microscopic contact area and friction between medical textiles and skin*. s.l. : Journal of the mechanical behavior of biomedical materials, 2014. pg. 114-125. Vol. 38.

54 **Diridollou, S, și alții. 2020.** *n vivo model of the mechanical properties of the human skin under suction*. s.l. : Skin Research and Technology, 2020. pg. 214-221. Vol. 6.

58 **Escoffier, C, și alții. 1989.** *Age-related mechanical properties of human skin: An in vivo study.* s.l. : The Journal of Investigative Dermatology, 1989. pg. 353-357. Vol. 93.

65 **Gao, C, Kuhlmann-Wilsdorf, D și Makel, D D. 1994.** *The dynamic analysis of stick-slip motion*. s.l. : Wear, 1994. pg. 1-12. Vol. 173(1).

66 **Gao, C, Kuhlmann-Wilsdorf, D și Makel, D. 1993.** *Fundamentals of stick-slip*. s.l. : Wear, 1993. pg. 1139-1149. Vol. 162.

71 **Gerhard, H și Vogel, M D. 1981.** *Directional variations of mechanical parameters în rat skin depending on maturation and age*. s.l. : The Journal of Investigative Dermatology , 1981. pg. 493-497. Vol. 76.

72 **Gerhardt, L C, și alții. 2008.** *Influence of epidermal hydration on the friction of human skin against textiles*. s.l. : Journal of the Royal Society Interface, 2008. pg. 1317-1328.

76 **Goryacheva, I G și Makhovskaya, Y Y. 2010.** *Modeling of friction at different scale levels*. s.l. : Modeling of friction at different scale levels, 2010. pg. 390-398. Vol. 45(3).

77 **Grahame, R. 1969.** *Elasticity of human skin in vivo*. s.l. : Annals of physical medicine, 1969. pg. 130-134. Vol. 10.

93 **Jacquet, E, și alții. 2008.** *A new experimental method for measuring skin's natural tension*. s.l. : Skin Research and Technology, 2008. pg. 1-7. Vol. 14.

97 **Johnson, K L și Greenwood, J A. 1997.** *An adhesion map for the contact of elastic spheres*. s.l. : Journal of Colloid and Interface Science, 1997. pg. 326-333. Vol. 192(2).

104 **Khatyr, F, Imberdis, C, Vescovo, P, Varchon, D, Lagarde, JM.** *Model of the viscoelastic behaviour of skin in vivo and study of anisotropy,* Skin Research and Technology 2004; 10: 96–103

123 **Lui, Z și Yeung, K. 2008.** *The preconditioning and stress relaxation of skin tissue*. s.l. : Journal of Biomedical and Pharmaceutical Engineering, 2008. pg. 22-28. Vol. 3.

131 **Matsumura, H, și alții. 2001.** *Preconditioning of the distal portion of a rat random-pattern skin flap*. s.l. : British Journal of Plastic Surgery, 2001. pg. 58-61. Vol. 54.

140 **Mosteller, RD. 1987.** *Simplified calculation of body-surface area,* N Engl J Med. 1987 Oct 22;317(17):1098. doi: 10.1056/NEJM198710223171717. PMID: 3657876.

144 **Nakano K, Maegawa S. 2009a** *„Occurrence limit of stick-slip: dimensionless analysis for fundamental design of robust-stable systems", Lubr. Sci., vol. 22, pp. 1-18.*

162 **Pereira, J M, Mansour, J M și Davis, B R. 1991.** *Dynamic measurement of the viscoelastic properties of skin*. s.l. : Journal of Biomechanics, 1991. pg. 157-162. Vol. 24.

164 **Baumberger, T. 1995.** *Dry friction Dynamics at low velocities*. s.l. : Physics of Sliding Friction, Springer, 1995.

169 **Richard LG. 2017.** *Human Skin Is the Largest Epithelial Surface for Interaction with Microbes,* Journal of Investigative Dermatology, Volume 137, Issue 6, 2017, Pages 1213-1214, ISSN 0022-202X

171 **Sanders, R. 1973.** *Torsional Elasticity of Human Skin in-Vivo*. s.l. : Pflugers Archiv-European Journal of Physiology, 1973. pg. 255-260. Vol. 342.

175 **Soldatenkov, I. A., 2008,** *Calculation of the Deformation Component of the Force of Friction for a Standard Elastoviscous Base, ISSN 1068-3666, Journal of Friction and Wear, 2008, Vol. 29, No. 1, pp. 7–14.*

179 **Stark, H L. 1977.** *Directional variations în the extensibility of human skin.* s.l. : British Journal of Plastic Surgery, 1977. pg. 105-114. Vol. 30.

182 **Tabor, D. 1977.** *Surface forces and surface interactions.* s.l. : Journal of Colloid and Interface Science, 1977. pg. 2-13. Vol. 58(1).

203 **Wensrich, C. 2006.** *Slip-stik motion in harmonic oscillation chain subject to Coulomb friction.* s.l. : Tribology International, 2006. pg. 490-495. Vol. 39.